INFRARED SPECTRA OF GLASSES IN THE $15Na_2O.10(MgO,CaO,TiO_2,ZrO_2).75SiO_2$ SYSTEM

MAREK LIŠKA, HANA HULÍNOVÁ, PETER ŠIMURKA, JOZEF ANTALÍK*

Institute of Inorganic Chemistry, Slovak Academy of Sciences, Martina Rázusa 10, SK - 911 01 Trenčín, Slovak Republic (e-mail: liska@uach1.savba.sk)
**Department of Physical Chemistry, Faculty of Chemical Technology, Slovak Technical University, Radlinského 9, SK - 812 37 Bratislava,* Slovak Republic

Received 8. 8. 1994

The shape of infrared spectra measured by KBr pellet technique is characterized by very strong asymmetric peak with maximum at 996-1072 cm^{-1}, medium peak at 774-786 cm^{-1} and strong absorbance peak at 447-466 cm^{-1}. The maxima positions of the first and the third absorption peaks correlate linearly with the NBO/T ratio (i.e. non-bridging oxygen to tetrahedral central atom molar ratio), which depends on the presupposed value of the network-forming fraction of Ti atoms $\alpha_4(Ti)$. The correlation coefficient reaches maximal value for $\alpha_4(Ti)=0.15$ for the first peak and for $\alpha_4(Ti)=0.25$ for the third peak, confirming such way the partial network-forming activity of TiO_2. The spectral shape is explained by the superposition of $Q^4(SiO_2$; 3-dimensional), $Q^3(Si_2O_5$; sheet) and $Q^2(SiO_3$; chain) structural units. The spectra of Q^4 and Q^3 units obtained from measured spectra by linear regression analysis are in qualitative agreement with the results of numerical FG simulation of Furukawa et al.

INTRODUCTION

Multicomponent silicate glasses containing zirconia play dominant role in the research and development of alkali-resistant glass fibres for portland cement composites [1]. Among other oxides, the titanium dioxide is often present in these glasses for the sake of alkaliresistance improvement [2]. The knowledge of structure-composition relationships is the basic prerequisit allowing the efficient glass chemical composition optimization with respect to prescribed target physico-chemical properties. However, the quantitative description of TiO_2 structural role in multicomponent oxide glasses is still an open question. The results obtained using various methods, in particular various kinds of spectroscopy on one side (e.g. Raman, IR, XPS, EXAFS, XANES, neutron scattering...) and the analysis of proper physical properties (parcial molar volumes and refractivities, phase diagrams, viscosity and viscous flow activation energy...) on the other one, are often contradictory [3].

In our previous paper [4], the compositional dependencies of viscosity and viscous flow activation energy of $15Na_2O.10(MgO,CaO,TiO_2,ZrO_2).75SiO_2$ glasses have been studied. From the correlation between these quantities and the NBO/T value it was concluded that about 45 mol.% of TiO_2 acts as network-former. This particular value is an effective average characteristic for the compositional space studied.

The present study deals with the infrared spectra of the same set of glasses. Unlike in the Raman spectroscopy, the full quantitative interpretation of infrared spectra, especially of those obtained by KBr technique, is not possible. On the other hand, useful structural information may be obtained from the dependencies of peak maxima positions and relative intensities on glass composition and/or other quantities dependent of composition. Using these tools we have tried to quantify the average degree of network-forming activity of titanium dioxide.

EXPERIMENTAL

Batches were prepared from glass sand, zirconium silicate and chemically pure TiO_2, Na_2CO_3, $MgCO_3$ and $CaCO_3$ and melted in a Pt-10%Rh crucible between 1500 and 1550 °C. Homogeneity was ensured by repeated fritting and hand-mixing of the glass during melting. Each melt was poured from the crucible onto a stainless steel plate. The samples were tempered in a muffle furnace at 600 °C for one hour, after which the furnace was switched off and samples allowed to remain there until completely cool.

The chemical compositions of individual samples were determined by ICP emission spectral analysis after the samples had been decomposed by melting with lithium tetraborate.

The range of investigated compositions was delineated by a configurational tetrahedron with apices C, T, Z and M corresponding to melts with the following mol.% compositions:

C: 10CaO, $0TiO_2$, $0ZrO_2$, 0MgO, $15Na_2O, 75SiO_2$
T: 0CaO, $10TiO_2$, $0ZrO_2$, 0MgO, $15Na_2O, 75SiO_2$
Z: 0CaO, $0TiO_2$, $10ZrO_2$, 0MgO, $15Na_2O, 75SiO_2$
M: 0CaO, $0TiO_2$, $0ZrO_2$, 10MgO, $15Na_2O, 75SiO_2$

The chemical compositions together with the samples numbering convention and abbreviations are summarized in Table I.

Infrared spectra were measured with Pye Unicam PU9512 spectrometer with on line computer data collection. The transmittance data were sampled at room temperature with constant wavenumber step of 2 cm^{-1} in the range from 300 cm^{-1} to 1500 cm^{-1}. Two KBr pellets were prepared for each glass composition through mixing of 300 mg KBr with approximately 0.6 and 1.2 mg of glass powder. Finally the absorbance spectra were obtained averaging these two transmittance spectra converted to absorbance and rescaled to the 1 mg glass/300 mg KBr concentration. Figure 1 illustrates this procedure for six glass compositions. The differences between the absorbance spectra rescaled to 1 mg glass/300 mg KBr dilution (dashed lines) may be accounted for by the inaccuracy of weighting and ambient humidity influence.

The positions of peak maxima were found using the quadratic least squares fit in 7-points floating window.

The first and the second moments were calculated by the numerical integration between the limits given by the minima between the adjacent peaks or by the wavelength range limits (i.e. 300 and 1500 cm^{-1}). The positions of peak maxima along with the first and the second moments are summarized in Table II.

Table I. Chemical composition of studied glasses in mol.%

No	Glass	Na_2O	CaO	MgO	ZrO_2	TiO_2	SiO_2
1	CTZ01	14.60	10.48	0.00	0.00	0.00	74.92
2	CTZ02	14.55	0.00	0.00	0.00	9.26	76.19
3	CTZ03	15.35	0.00	0.00	9.78	0.00	74.87
4	CTZ04	15.13	5.20	0.00	5.09	0.00	74.58
5	CTZ05	14.69	5.23	0.00	0.00	4.90	75.18
6	CTZ06	14.92	0.00	0.00	4.59	4.82	75.67
7	CTZ07	14.40	3.20	0.00	3.20	3.50	75.80
8	CTZ08	14.93	6.93	0.00	2.50	0.00	75.64
9	CTZ09	15.09	2.32	0.00	7.38	0.00	75.22
10	CTZ10	14.83	2.42	0.00	0.00	7.18	75.57
11	CTZ11	14.95	7.45	0.00	0.00	2.50	75.10
12	CTZ12	14.52	0.00	0.00	2.52	7.22	75.74
13	CTZ13	14.74	0.00	0.00	7.73	2.39	75.14
14	CTZ14	14.61	2.55	0.00	4.61	2.15	76.08
15	CTZ15	14.68	4.64	0.00	2.01	2.25	76.43
16	CTZ16	15.04	2.34	0.00	2.13	4.70	75.79
17	CTZM04	14.43	0.00	9.57	0.00	0.00	75.99
18	CTZM09	14.54	0.00	5.40	0.00	6.06	74.00
19	CTZM10	14.72	0.00	5.27	5.02	0.00	74.99
20	CTZM13	14.79	2.62	7.58	0.00	0.00	75.01
21	CTZM15	14.34	0.32	8.08	0.00	2.52	74.74
22	CTZM16	15.01	0.00	7.94	2.55	0.00	74.50
23	CTZM21	14.76	0.00	2.74	0.00	7.99	74.50
24	CTZM22	15.02	0.00	2.73	7.61	0.00	74.65
25	CTZM24	14.26	5.36	2.54	0.00	2.48	75.36
26	CTZM27	14.80	2.71	2.71	0.00	5.25	74.53
27	CTZM29	14.45	2.77	5.33	0.00	2.54	74.91
28	CTZM30	15.12	2.47	2.65	5.00	0.00	74.75
29	CTZM32	14.71	0.00	2.32	2.38	5.16	75.43
30	CTZM33	14.57	0.00	2.37	5.11	2.39	75.57
31	CTZM34	14.79	0.00	4.58	2.50	2.39	75.75

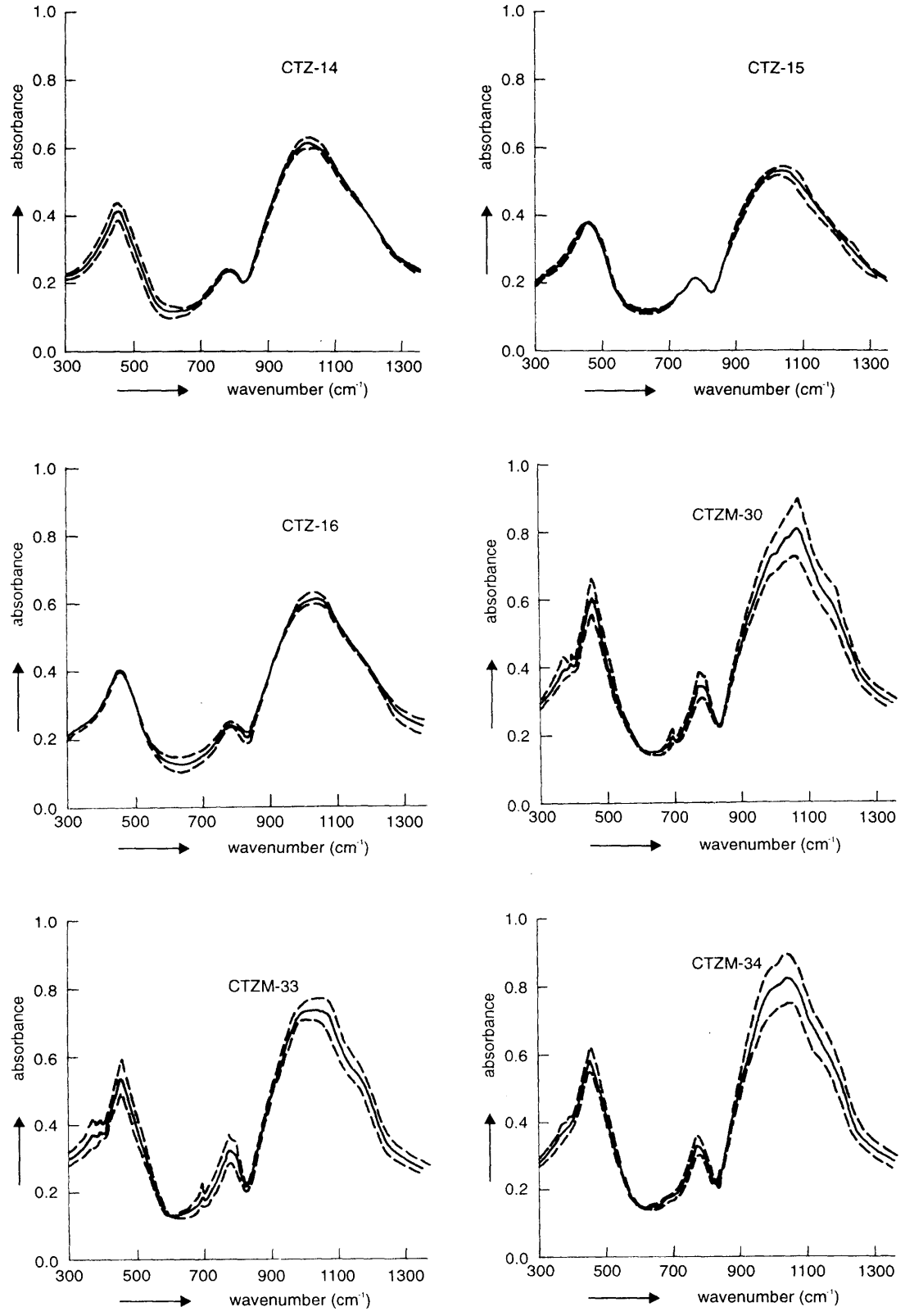

Figure 1. The absorbance spectra at two different dilution of glass powder in KBr after rescaling to the concentration of 1 mg glass/300 mg KBr (dashed lines) and the average spectrum used in this paper (full line)

Table II. The positions of peak maxima (h1c,h2c,h3c (cm^{-1})) along with the first (av1,av2,av3 (cm^{-1})) and second (s21, s22,s23 (cm^{-2})) moments of IR absorbance spectra

Glass	h1c	av1	s21	h2c	av2	s22	h3c	av3	s23
CTZ01	466	443	4655	778	731	4520	1056	1105	19941
CTZ02	455	446	6527	786	739	3369	1051	1093	21263
CTZ03	447	439	5539	782	725	4437	1005	1084	21077
CTZ04	460	445	4514	774	727	4591	1030	1089	19697
CTZ05	461	441	5760	780	740	3568	1050	1096	20592
CTZ06	454	435	5268	780	733	4043	1000	1081	19769
CTZ07	458	439	5405	779	732	3920	1021	1084	20006
CTZ08	461	440	5012	774	722	4596	1039	1094	20955
CTZ09	456	450	6496	778	740	3034	1016	1086	20325
CTZ10	459	453	7296	781	745	2696	1055	1091	20801
CTZ11	463	443	5505	777	736	3767	1042	1104	21505
CTZ12	455	458	7761	782	744	2623	1036	1087	20715
CTZ13	452	448	6780	778	737	3148	996	1084	21432
CTZ14	457	446	6068	784	737	3398	1019	1090	20487
CTZ15	460	450	6539	777	740	2985	1037	1090	20550
CTZ16	460	449	6356	782	737	3304	1040	1089	20465
CTZM04	462	457	6822	778	750	2592	1049	1100	19645
CTZM09	460	452	6583	781	746	3015	1053	1092	19478
CTZM10	458	447	5881	777	736	3631	1022	1086	19589
CTZM13	463	456	6042	778	746	3011	1050	1096	17856
CTZM15	462	452	5899	780	740	3621	1058	1099	18974
CTZM16	458	448	5893	777	736	3752	1045	1094	19498
CTZM21	457	439	5419	779	727	4507	1006	1086	20419
CTZM22	452	440	5440	782	728	4282	999	1081	19908
CTZM24	462	452	6473	778	747	2777	1053	1093	19421
CTZM27	461	453	6898	784	750	2753	1048	1090	19225
CTZM29	460	456	7229	777	752	2536	1040	1096	19949
CTZM30	458	449	6593	777	746	2874	1072	1093	19493
CTZM32	458	450	6565	778	741	2982	1037	1084	19432
CTZM33	456	440	5632	776	732	3799	1026	1085	19881
CTZM34	459	447	5996	777	738	3362	1049	1089	19310

RESULTS AND DISCUSSION

The infrared spectra of glasses with C, T, Z and M compositions are compared in Figure 2. We can see that the spectra are qualitatively similar, namely in the region of the first two peaks. The differences in the relative intensity of the second peak are due to the changes in the low frequency branch of the third peak. The weak, but discernible shoulder at approximately 940-950 cm^{-1} is present in all the spectra. The third peak maxima positions are close for the C, T and M glasses (1049-1056 cm^{-1}) unlike the Z glass with the peak maximum at 1005 cm^{-1}. Despite the narrow region close to the maximum the overall shape of Z and M third peaks is very similar. On the other hand the third peak of T glass (C glass) is extremly broad (narrow) when compared with those of Z and M glasses. The medium shoulder at 1140-1150 cm^{-1} may be distinguished in high frequency branch of the third peak in all the spectra.

The main spectral features may be accounted for realizing the prevalent role of Si-O network vibrations in the frequency region studied. The basic spectral shape is implied by the 75 mol.% SiO_2 and 15 mol.% Na_2O present in all the glass samples. The C a M samples correspond to mixed alkali - alkaline earth oxide trisilicate glass compositions. The structure of such glasses is built of Q^4, Q^3 and Q^2 SiO_4 tetrahedral structural units. Here Q^4 stands for fully polymerized SiO_4 tetrahedra with 4 bridging oxygens (BO), Q^3 corresponds to sheet structural unit with one non-bridging oxygen (NBO) and Q^2 represents the chain unit with two NBOs. Furukawa et al. [5] have calculated the frequencies and the relative intensities of infrared spectra of individual Q-units. The spectra obtained for Q^4 and Q^3 units supposing the same FWHM (full width at half maximum) of 200 cm^{-1} for all the spectral peaks are illustrated in Figure 3. The three observed composite peaks may be assigned to Si-O stretching (near 1000 cm^{-1} and 800 cm^{-1}) and to com-

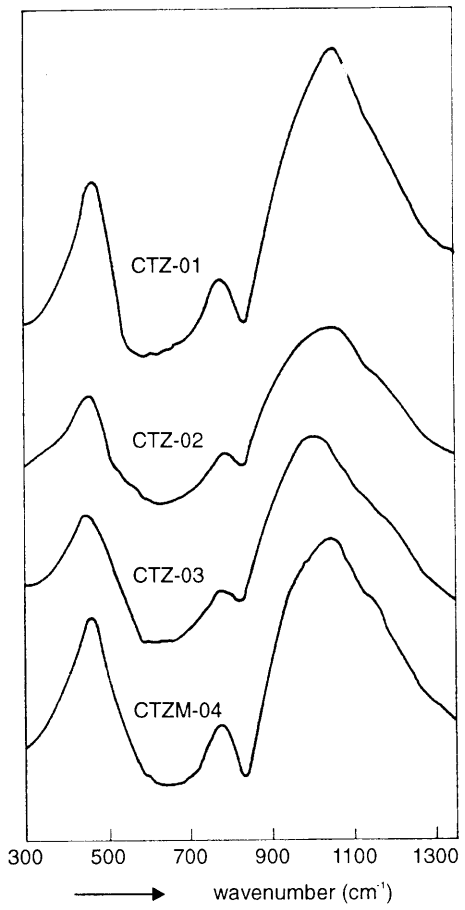

Figure 2. Infrared absorbance spectra of C (CTZ-01), T (CTZ-02), Z (CTZ-03) and M (CTZM-04) glasses

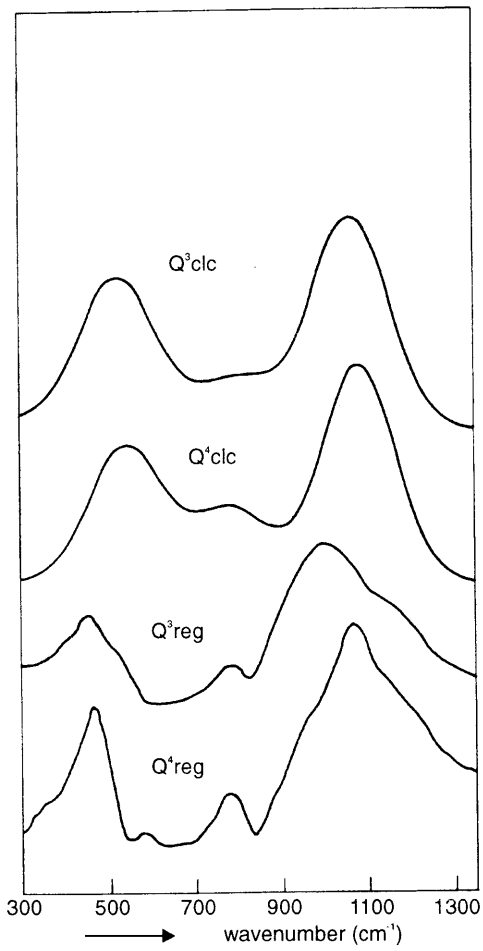

Figure 3. Infrared absorbance spectra of Q^4 and Q^3 structural units:
- obtained from FG analysis [5] by supposing 200 cm^{-1} FWHM for all the spectral components (Q^4_{clc},Q^3_{clc});
- obtained from our least squares regression (Q^4_{reg},Q^3_{reg})

bined Si-O-Si bending - Si-O stretching (near 470 cm^{-1}) vibrations.

The relative abundances of individual Q-units may be calculated using the approximate regression formulae obtained from Raman spectroscopy structural investigations of Mysen [3]. The mole fractions of Q-units are expressed as fourth degree polynomials of stoichiometric NBO/T calculated from the oxide glass compositions. The distinct quality of charge balancing cations is reflected in the idividual sets of polynomial coefficients for Na_2O, K_2O, MgO, CaO and FeO. The Q-distribution is determined through the weighted average in the case of multicomponent glasses. Unfortunately, ZrO_2 and TiO_2 oxides are not included in this parametrization.

In the case of zirconia, the modifying role of Zr^{4+} cation which is present with 7-8 coordination in the glass structure [6] allows us to presume similar spectral features as in the case of alkaline earth oxides of strong field cations. The stoichiometric constraints must be of course respected giving the equivalency of two moles of alkaline earth oxide with one mole of ZrO_2 (because these quantities produce the same number of NBOs). However the interactions of heavy Zr^{4+} cations with the silicate network cause the shift of (especially stretching) vibration modes to lower wavelengths.

Unlike zirconium, titanium(IV) ions can enter the glass structure with both four-fold coordination acting as network-former and six-fold coordination corresponding to modifying function. The spectral features of the network-modifying part of TiO_2 are thus comparable with the stoichiometrically equivalent amount of rare earth oxides. Moreover, the TiO_6 F_{1u} vibration modes at 335 cm^{-1} (bending) and 570 cm^{-1} (stretching) are observed in the IR spectrum [7]. These may be seen as weak shoulders on both sides of the first peak of T-composition spectrum (Figure 2). On the other hand, the tetrahedral network-forming part of TiO_2 produces IR spectral peak at 940 cm^{-1} [8]. This peak coincides with the 941 cm^{-1} peak of Si-NBO stretching vibration.

The overall polymerization of the glass is solely determined by the NBO/T ratio. Providing that $\alpha_4(Ti)$ fraction of the total amount of TiO_2 acts as network-former, the following relation between the glass composition and NBO/T ratio may be obtained

$$NBO/T = 2\{[1-2\alpha_4(Ti)]x(TiO_2) + x(ZrO_2)-x(SiO_2) + 1\}/$$
$$/[\alpha_4(Ti)x(TiO_2) + x(SiO_2)] \quad (1)$$

where $x(i)$ is the mole fraction of the oxide i. In the set of studied glasses the maximum NBO/T value of 0.93 was reached for $x(ZrO_2) = 0.1$ and $x(SiO_2) = 0.75$.

For NBO/T ranging from 0 to 0.9 only the Q^4, Q^3 and Q^2 units are present in significant amounts with stoichiometrically constrained relative abundances:

$$x(Q^4) + x(Q^3) + x(Q^2) = 1$$
$$x(Q^3) + 2x(Q^2) = NBO/T \quad (2)$$

the latter equation reflecting the stoichiometry of disproporciation reaction

$$2Q^3 = Q^4 + Q^2 \quad (3)$$

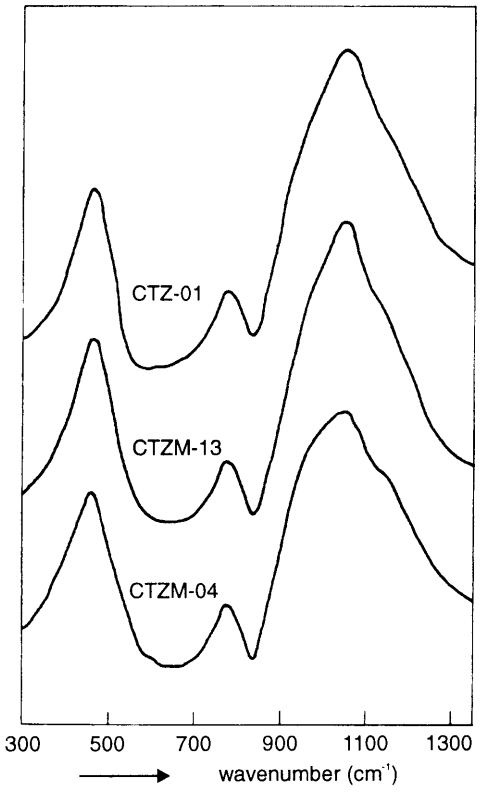

Figure 4. IR absorbance spectra of glasses in which MgO was stepwise substituted for CaO:
CTZ-01(10.5 mol.% CaO, 0.0 mol.%MgO),
CTZM-13(2.6 mol.%CaO, 7.6 mol.%MgO),
CTZM-04(0.0 mol.%CaO, 9.6 mol.%MgO)

The influence of modifying cation type on Q-units distribution may be generalized in terms of its field strength (quantified by the ratio Z/r^2 = charge/squared radius). The abundances of 3-dimensionally interconnected network units $x(Q^4)$ and chain unit $x(Q^2)$ are positively correlated with cations Z/r^2 whereas $x(Q^3)$ decreases with increasing Z/r^2.

The shift of individual silicate anions Si-O stretching vibrations towards lower wavenumbers accompanied with increasing number of NBO (i.e. with decreasing polymerization degree) was predicted by the theoretical FG analysis of Furukawa et al.[5] and experimentally confirmed in the work of Taniguchi [9].

Combining the last rule with the Q-distribution dependance on cation field strength some compositional trends in the high frequency composed peaks of measured spectra may be explained.

The effect of MgO substitution for CaO is illustrated in Figure 4. The broadening of Q-distribution by increasing the cation field strength ($Q^4+Q^3->Q^4+Q^3+Q^2$) is reflected in corresponding broadening of the high frequency peak accompanied with small shift of its maximum to lower wavenumbers.

Figure 5 demonstrates the series of spectra obtained by substitution of ZrO_2 for MgO. It can be seen, that the entire third peak is significantly (of 44 cm^{-1}) shifted to lower wavenumbers. This shift may be accounted for by combined effect of decrease of overall polymerization degree (1 ZrO_2 corresponds to 2 MgO) and by the heavy Zr^{4+} ion "dumping" effect on Si-O...Zr stretching vibrations. In addition the greater Zr^{4+} field strength causes the broadening of Q-distribution thus enhancing the peak width.

Similar effects with the same possible explanation are present in the spectral series for CaO <- ZrO_2 substitution illustrated in Figure 6. Because of smaller Ca^{2+} field strength (compared with Mg^{2+}) the Q-distribution broadening effect is more pronounced in this case.

Only the substitutions between the network-modifying oxides have been discussed until now. The situation becomes more complex when we include titanium dioxide with both the network-forming and network-modifiying activities. Figure 7 shows such substitution between MgO and TiO_2. Referring to the results of other works [3,4,8] we expect the network-modifying activity to preveal at lower TiO_2 concentrations and vice versa. Indeed going from Ti-free M-glass to the glass with 2.5 mol.% TiO_2 we can see some narrowing and simplifying of spectral shape implied by the enhancing of polymerization degree accompanied with the narrowing the Q-distribution. Increasing the TiO_2 content up to 5 mol.% returns the spectrum back to the broad fashion. Going on to 10 mol.% of TiO_2, the additional broadening associated with significant shift to

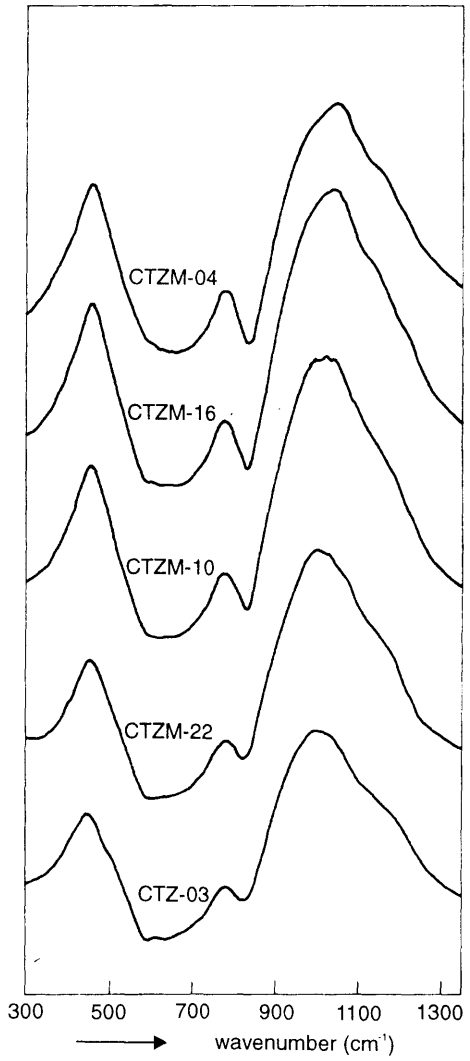

Figure 5. IR absorbance spectra of glasses in which ZrO_2 was stepwise substituted for MgO:
CTZM-04(9.6 mol.%MgO, 0.0 mol.%ZrO_2),
CTZM-16(7.9 mol.%MgO, 2.6 mol.%ZrO_2),
CTZM-10(5.3 mol.%MgO, 5.0 mol.%ZrO_2),
CTZM-22(2.7 mol.%MgO, 7.6 mol.%ZrO_2),
CTZ-03(0.0 mol.%MgO, 9.8 mol.%ZrO_2)

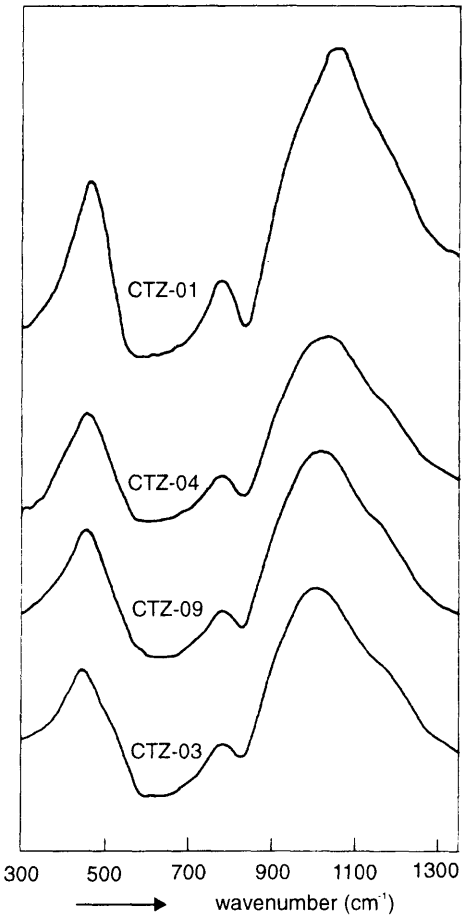

Figure 6. IR absorbance spectra of glasses in which ZrO_2 was stepwise substituted for CaO:
CTZ-01(10.5 mol.% CaO, 0.0 mol.%ZrO_2),
CTZ-04(5.2 mol.% CaO, 5.1 mol.%ZrO_2),
CTZ-09(2.3 mol.% CaO, 7.4 mol.%ZrO_2),
CTZ-03(0.0 mol.% CaO, 9.8 mol.%ZrO_2)

lower wavenumbers can be seen, both these effects being caused by the network-modifying activity of TiO_2. Moreover, the weak shoulders at both sides of the first peak (at approx. 335 cm^{-1} and 570 cm^{-1}) typical to F_{1u} vibrations of TiO_6 group are present in this spectrum.

Similar situation is met at Figure 8, where the spectral series for CaO <- TiO_2 substitution is shown. Here the starting titania-free spectrum is narrower for the greater electropositivity of Ca as compared to Mg. Therefore the initial narrowing connected with network-forming activity of TiO_2 is absent in the spectrum of the glass with 2.5 mol.% TiO_2. In addition, the transformation of TiO_4 to TiO_6 was observed [8] with increasing Na_2O content in the Na_2O-TiO_2-SiO_2 glasses. This fact may be extrapolated to the conclusion that the extent of this transfer to network-modifying TiO_2 form is proportional to the network-modifying ability of particular aklali or alkaline earth oxide. Thus in this glass series (Figure 8) the average network-forming activity of TiO_2 is expected to be lower than in the case of MgO<-TiO_2 substitution (Figure 7). The TiO_6 shoulders at the first peak are also discernible in the case of 7.5 mol.% of TiO_2.

The above results pointed out the dependance of the amount of network-forming TiO_2 form on both the TiO_2 content and the quality and concentration of other network-modifying oxides present in the glass. It is thus obvious that using a single constant α_4(Ti) value for the network-forming TiO_2 fraction is only a crude (but useful) approximation. Therefore the numerical values of

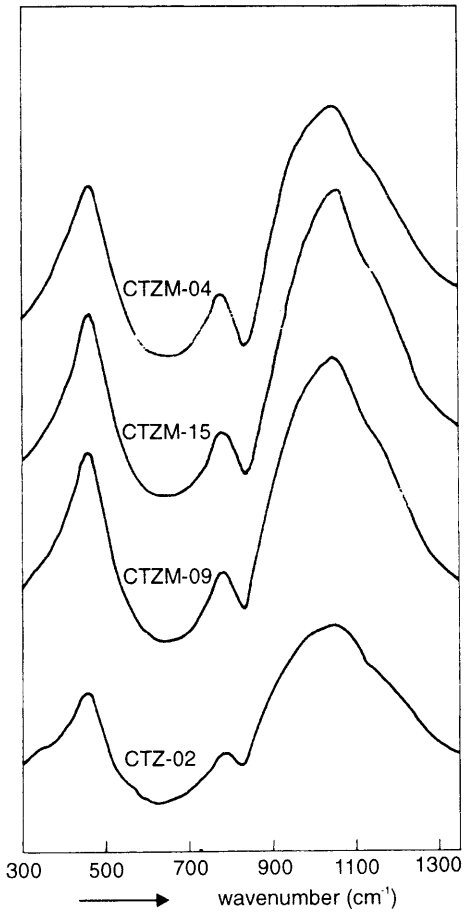

Figure 7. IR absorbance spectra of glasses in which TiO_2 was stepwise substituted for MgO:
CTZM-04(9.6 mol.% MgO, 0.0 mol.% TiO_2),
CTZM-15(8.1 mol.% MgO, 2.5 mol.% TiO_2),
CTZM-09(5.4 mol.% MgO, 6.1 mol.% TiO_2),
CTZM-21(2.7 mol.% MgO, 8.0 mol.% TiO_2),
CTZ-02(0.0 mol.% MgO, 9.3 mol.% TiO_2)

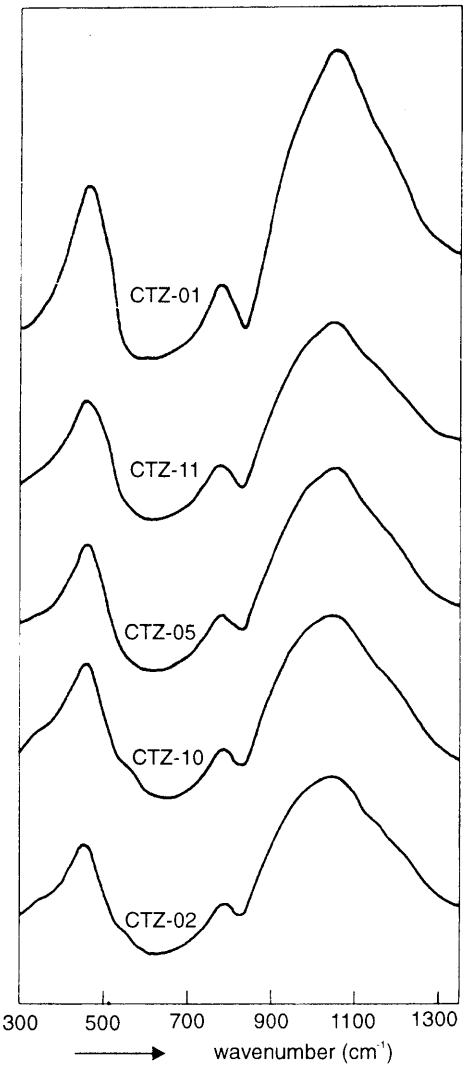

Figure 8. IR absorbance spectra of glasses in which TiO_2 was stepwise substituted for CaO:
CTZ-01(10.5 mol.% CaO, 0.0 mol.% TiO_2),
CTZ-11(7.5 mol.% CaO, 2.5 mol.% TiO_2),
CTZ-05(5.2 mol.% CaO, 4.9 mol.% TiO_2),
CTZ-10(2.4 mol.% CaO, 7.2 mol.% TiO_2),
CTZ-02(0.0 mol.% CaO, 9.3 mol.% TiO_2)

α_4(Ti) estimated using various physical quantities and/or various sample sets may substantially differ from each other. Keeping this fact in mind we have investigated the correlations between the NBO/T value calculated supposing certain constant α_4(Ti) value on one side and various spectral characteristics (like peaks maxima positins, first and second peaks moments etc.) on the other.

The most significant correlations were obtained for the peak maxima positions of the first and the third peak. Both these correlations were evaluated for continuously varying values of α_4(Ti). The values of correlation coefficient r and coefficient of determination R^2 (i.e. % of explained variance) versus α_4(Ti) are plotted in Figures 9 and 10 for the first and the third peak, respectively. Only the glasses with nonzero TiO_2 or ZrO_2 content were included in the regression treatment. For the first peak both coefficients reached broad local maximum at α_4(Ti)≈0.15 yielding the values r_{max}=0.88 and R^2_{max}=78%. The maximum values r_{max}=0.70 and R^2_{max}=49% were obtained at α_4(Ti)≈0.20 for the third peak. Comparing these results with other α_4(Ti) estimates it can be concluded that they are both lower than:

- the α_4(Ti)≈0.5 value obtained by Yamanaka from oxygen 1s XPS spectroscopy [10] of $x$$Na_2O.y$$TiO_2.(1-x-y)SiO_2$ (x=0.2 and 0.3 and y=0-0.35) glasses;
- the α_4(Ti)≈0.45 value obtained in our previous study [4] from compositional dependencies of viscosity and viscous flow activation energy of the same set of glasses as in the present paper.

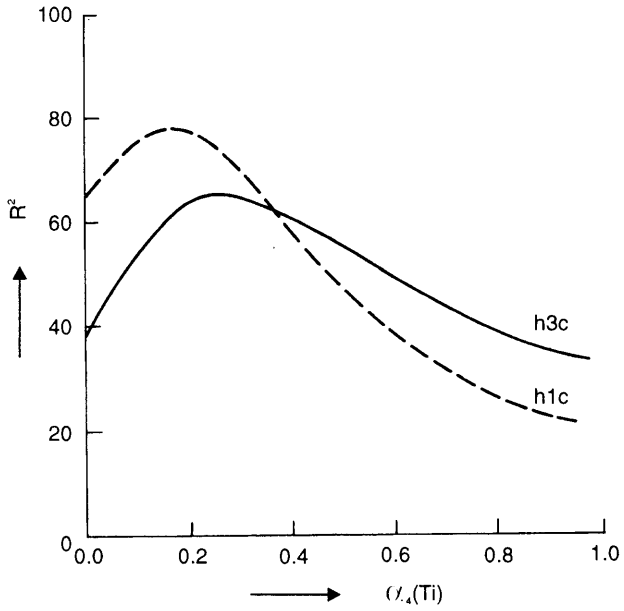

Figure 9. Coefficient of determination R^2 of the first/third peak maximum (h1c/h3c) dependance on NBO/T plotted versus the presupposed value of netwotk-forming fraction of TiO_2

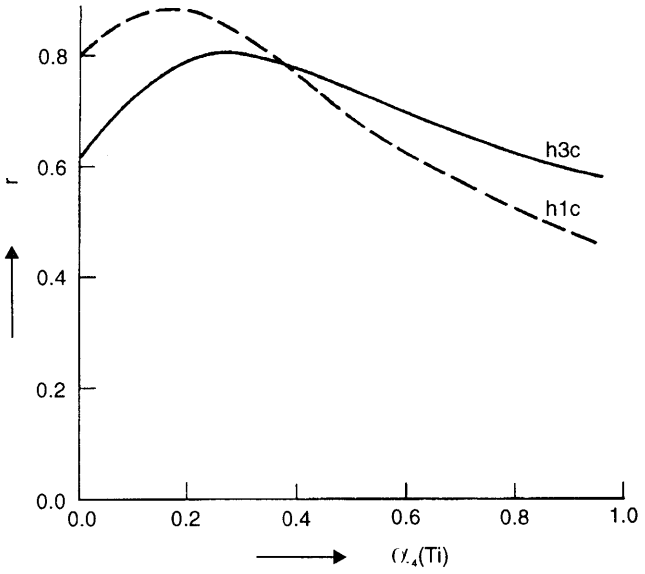

Figure 10. Correlation coefficient r of the first/third peak maximum (h1c/h3c) dependance on NBO/T plotted versus the presupposed value of netwotk-forming fraction of TiO_2

It may be concluded that the results of the above regression analysis confirm the simultaneous network-forming and network-modifying activities of TiO_2. However, some spectral features of network-forming tetrahedra TiO_4 (esp. ~940 cm^{-1} absorption) overlap with the spectral manifestation of network-modifying oxides (esp. ~941 cm^{-1} absorption of Si-NBO), thus the numerical results obtained are only rough approximation. Also the "dumping" effect of heavy Zr^{4+} ions makes the correlation relatively vague. This is true predominantly for the third (stretching) peak where the correlation characteristics are significantly lower than for the first (stretching-bending) one.

Preliminary correlation analysis pointed out strong dependancies between the mole fractions of Q-motives calculated according to Mysen [3] using the Fe(II) parameters of regression polynomial for both the unknown parameters of Ti(IV) and Zr(IV). This crude approximation was used only in the first step to show why the straightforward regression isolation of individual Q^n (n = 4, 3, 2) spectra from experimental IR spectra is not possible.

In the next step we neglected the Q^3 disproporciation reaction (it means we suppose the equilibrium (4) to be shifted to the left) resulting in $x(Q^2) = 0$. Then the mole fractions $x(Q^4)$ and $x(Q^3)$ were simply determined from stoichiometry according to Equations (2, 3). Using the standard linear regression analysis the least squares problem has been solved for the evaluation Q^3 and Q^4 individual spectra. The solution is presented in Figure 3 (curves Q^4_{reg} and Q^3_{reg}) together with the spectra constructed from Furukawa [5] FG analysis results (curves Q^4_{clc} and Q^3_{clc}). Comparing the spectra, it can be concluded that the ones obtained by linear regression analysis are in qualitative accord with the results of numerical FG simulation. This result is only qualitative one, but as such can confirm the basic idea that the main spectral manifestation of compositional changes of the glasses studied resides in changes of relative abundance of Q-units.

CONCLUSIONS

Infrared spectra of the glasses studied reflect the changes of relative abundances of Q^4, Q^3 and Q^2 structural units in dependance on the quality and content of modifying oxides involved in the glass. The spectra of Q^4 and Q^3 structural units determined by regression analysis are in qualitative agreement with the theoretical results of Furukawa et al. [5].

The spectral shape changes caused by the variation of relative amounts of Na_2O, CaO and MgO agree with the previously established correlations between Q-units mole fractions and modifying cations electropositivity.

The fully modifying activity of ZrO_2 was confirmed. Both the network-forming and network-modifying activities of TiO_2 were detected on the basis of the spectral shape changes analysis as well as from the correlation

analysis of peak maxima position dependance on NBO/T. This principal result is in harmony with the results of previous investigations studying the other physical properties (XPS spectroscopy, viscosity) and/or other glass compositions systems.

Acknowledgement

This work was supported by the Slovak Grant Agency for Science under the grant number 1171/94.

References

1. A.J.Majumdar, J.F.Ryder: Glass Technol. *9*, 78 (1968).
2. A.Plško, P.Lichvár, P.Šimurka: Silikáty *31*, 255 (1987).
3. B.O.Mysen: *Structure and properties of silicate melts*, Elsevier, New York 1988.
4. M.Liška, P.Šimurka: Phys. Chem. Glasses *36*, 6 (1995).
5. T.Furukawa, K.E.Fox, W.B.White: J. Chem. Phys. *75*, 3226 (1981).
6. P.P.Bihuniak, R.A.Condrate: J. Non-Cryst. Solids *44*, 331 (1981).
7. K.Kusabiraki, Y.Shiraishi: J. Japan Inst. Metals *45*, 259 (1981).
8. K.Kusabiraki: J. Non-Cryst. Solids *95&96*, 411 (1987).
9. H.Taniguchi: Tschemaks Mineral. Petrol. Mitteilungen *34*, 117 (1985).
10. H.Yamanaka, K.Nakahata, R.Terai: J. Non-Cryst. Solids *95&96*, 405 (1987).

Submitted in English by the authors

INFRAČERVENÉ SPEKTRÁ SKIEL SÚSTAVY $15Na_2O.10(MgO,CaO,TiO_2,ZrO_2).75SiO_2$

MAREK LIŠKA, HANA HULÍNOVÁ, PETER ŠIMURKA, *JOZEF ANTALÍK

Ústav anorganickej chémie Slovenskej akadémie vied, Dúbravská cesta 9, 842 36 Bratislava
**Katedra fyzikálnej chémie Slovenskej technickej univerzity, Radlinského 9, 812 37 Bratislava*

Skúmalo sa 31 zložení skiel uvedenej sústavy (Tabulka 1) pripravených tavením zo základných oxidov a uhličitanov v platinoródiových kelímkoch v okolitej atmosfére.

Infračervené (IČ) spektrá sa on line snímali s krokom 2 cm^{-1} na spektrometri Pye Unicam 9512 v rozsahu 300 cm^{-1} 1500 cm^{-1} pri dvoch rôznych zriedeniach práškových vzoriek skla v KBr tabletkách.

Tvar IČ spektier je charakterizovaný silným asymetrickým absorpčným pásom s maximom pri 996-1072 cm^{-1}, stredným pásom pri 774-786 cm^{-1} a silným absorpčným pásom pri 447-466 cm^{-1}. Polohy maxím prvého a tretieho absorpčného pásu lineárne korelujú s pomerom látkových množstiev nemôstikových kyslíkov (NBO) a tetraédrických cetrálnych sieťotvorných katiónov T. Hodnota uvedeného pomeru (NBO/T) pritom závisí od predom zvolenej veľkosti relatívneho zastúpenia sieťotvornej formy oxidu titaničitého α_4(Ti). Korelačný koeficient dosahuje maximálnu hodnotu pre α_4(Ti)=0.15 (0.25) v prípade prvého (tretieho) pásu (Obr. 9,10). Takto sa potvrdila dvojitá funkcia TiO_2 v štruktúre uvedených skiel implikovaná v predchádzajúcich prácach z viskozitných meraní.

Tvar IČ spektier možno interpretovať ako superpozíciu Q^4(trojrozmerná sieť), Q^3(vrstva) a malého množstva Q^2(retiazka) štruktúrnych motívov. Spektrá štruktúrnych jednotiek Q^4 a Q^3 získané z nameraných IČ spektier regresnou analýzou sú v kvalitatívnej zhode s výsledkami FG analýzy Furukawu a spol.